Structure of Molecule-rich Chalcogenide Glasses along the Join P_4Se_3-As_4Se_3: Results from ^{77}Se and ^{31}P NMR and Raman Spectroscopy

[1]Bing Yuan, [2]Bruce G. Aitken, [3]Derrick C. Kaseman, [3]Ping Yu, [1]Sabyasachi Sen*

[1]Department of Materials Science & Engineering, University of California at Davis, Davis, CA 95616, USA

[2]Science & Technology Division, Corning Inc., Corning, NY 14831, USA

[3]Nuclear Magnetic Resonance Facility, University of California at Davis, Davis, CA 95616, USA

*Corresponding Author: Sabyasachi Sen (email: sbsen@ucdavis.edu)

ABSTRACT

The atomic structure of unusually molecule-rich glasses along the P_4Se_3-As_4Se_3 join with 0 to 70 mol% P_4Se_3 is studied using Raman, ^{77}Se magic-angle-spinning (MAS) and 2D ^{31}P phase adjusted spinning sideband (PASS) nuclear magnetic resonance (NMR) spectroscopy. When taken together, the spectroscopic results indicate the coexistence of cage-like $P_xAs_{4-x}Se_3$ molecular moieties and corner-shared P- and As- containing pyramidal network moieties in the structure of these glasses. Increasing substitution of As with P gives rise to a monotonic increase in the total molecule:network ratio, which is shown to be consistent with the compositional variation in the glass transition temperature.

1. INTRODUCTION

Chalcogenide glasses are well known for their remarkable optical properties such as wide infrared transparency and large refractive index and optical nonlinearity, which make them promising photonic materials for a wide range of applications including in telecommunication, remote sensing and switching [1–10]. The unique compositional flexibility of these glasses in the form of continuous alloying enables compositional engineering for the precise tuning of optical, electronic, and other physical properties. Therefore, a fundamental understanding of the compositional evolution of atomic structure of these glasses is crucial in building predictive models of their structure-property relationship. The short- and intermediate-range atomic structure of the archetypal glass-forming chalcogenide systems have been studied extensively in the literature, including but not limited to various binary and ternary Ge-As-P-S/Se/Te glasses. In most cases, As, Ge or P atoms act as crosslinkers of chalcogen (S/Se/Te) atoms to form three-dimensionally connected network structures [11–21]. On the other hand, the existence of predominantly molecular chalcogenide glasses with an unusually low degree of structural connectivity has also been reported in Ge/P-doped As-S and P-Se pseudo-binary systems near the stoichiometry of A_4B_3, where A = As or P and B = S or Se [11-18]. The structure of these glasses primarily consists of cage-like A_4B_3 molecules that contain a basal 3-membered A_3 ring surmounted by an apical AB_3 pyramid with each atom in the A_3 ring being bonded to one of the B atoms in the pyramid.

Both crystalline and amorphous molecular chalcogenides consisting of A_4B_3 molecules held together by weak van der Waals forces have received significant attention due to the unique properties associated with them. For example, all A_4B_3 molecular crystals undergo a phase transition to a plastic crystal phase upon heating where the molecules are fixed in their lattice

positions but are free to perform rotation, attesting to their nearly spherical shape and weak intermolecular bonding [22]. Consequently, the enthalpy and entropy of this phase transition in these molecular crystals are much larger than that of melting [22]. Although stoichiometric A_4B_3 molecular liquids do not form bulk glass upon quenching, compositions close to stoichiometry can be formed into predominantly molecular glasses in the case of As-S and P-Se systems on doping with Ge and P, respectively, such that molecular glasses of composition $(GeS_2)_x(As_4S_3)_{100-x}$ with $1 \leq x \leq 3$ and P_5Se_3 have been reported in the literature [18,23,24]. Similar to the crystals, the weak intermolecular bonding is also manifested in these glasses in their rather low glass transition temperature ($T_g < 40$ °C) and high thermal expansion coefficient (90-100 ppm/°C) [18]. Moreover, NMR spectroscopy and inelastic neutron scattering studies of these glasses indicated the presence of rapid rotational motion of the constituent molecules at temperatures well below T_g, at timescales that are decoupled from that of the shear relaxation by many orders of magnitude [18,24–27]. Finally, viscosity measurements on the parent liquids in their supercooled state indicated that these molecular liquids are characterized by a rather steep temperature dependence of viscosity as the temperature approaches T_g, thus displaying a "fragile" behavior [27–29]. In contrast to these As_4S_3 and P_4Se_3 based compositions, bulk glass can indeed be formed from a stoichiometric liquid of composition As_4Se_3. This difference in the behavior of the latter is consistent with the results of previous structural studies of As_4Se_3 glass, which indicated that its structure consisted of a relatively small fraction of As_4Se_3 molecules that are interspersed with a $As(As,Se)_3$ pyramidal network and two-dimensional clusters of homopolar bonded As atoms [16,17,30].

It is interesting to note that previous studies of the phase equilibria in these molecular chalcogenide crystals in ternary As-P-S/Se systems indicated the existence of a complete solid solution between As_4Se_3 and P_4Se_3 where P and As atoms randomly replace one another in the

molecule without any preference for the apical and the basal sites [22]. On the other hand, for crystals in the P-As-S system, the P atoms show a strong preference for the apical site in the constituent $(P,As)_4S_3$ molecules [22]. Although, as noted above, a number of structural and dynamical studies of molecular glasses in doped binary As-S and P-Se systems have been reported in the literature, such studies on molecule-rich ternary As-P-Se glasses have remained scarce [31]. Here we present the results of a structural investigation of glasses along the join As_4Se_3–P_4Se_3 with P_4Se_3 contents varying from 0 to 70 mol.% using a combination of Raman, ^{77}Se magic-angle spinning (MAS) and two-dimensional ^{31}P phase-adjusted spinning sideband (PASS) nuclear magnetic resonance (NMR) spectroscopy. The spectroscopic results allow the identification of mixed $P_xAs_{4-x}Se_3$ molecules in these chalcogenide glasses for the first time. The compositional evolution of the structure is shown to be consistent with the corresponding variation in T_g.

2. EXPERIMENTAL

2.1 Sample Synthesis and Physical Characterizations

The P_4Se_3-As_4Se_3 glasses with 0, 20, 40, 50, 60 and 70 mol% P_4Se_3 were prepared in ~ 12g batches from constituent elements using the conventional melt-quench method. Mixtures of red phosphorus (Spectrum, 99.999%), selenium (Alfa Aesar, 99.999%) and arsenic (Alfa Aesar, 99.999%) were taken in 8 mm inner diameter vacuum sealed quartz ampoules (10^{-4} Torr) and melted in a rocking furnace at 873 K for 36 h to ensure melt homogeneity. The ampoules were then quenched in water to obtain the glass samples. The T_g of these glasses was determined using differential scanning calorimetry (Mettler Toledo DSC1). Samples of mass ~15-20 mg were taken in hermetically sealed Al pans and were heated to 20 °C above T_g to erase any thermal history. The samples were then cooled in the calorimeter at a rate of 10K/min and subsequently reheated

at the same rate and T_g was determined as the onset of the glass transition endotherm during reheating. Experimental errors were obtained from multiple scans on the same sample using the same heating and cooling rate.

2.2.Raman Spectroscopy

The Raman spectra of all glasses were collected in backscattering geometry using a Renishaw 1000 Raman microscope spectrometer equipped with a He-Ne laser operating at a wavelength of 633 nm. The backscattered light was detected using a charge-coupled device cooled to 200 K.

2.3. NMR Spectroscopy

^{77}Se MAS and 2D ^{31}P PASS NMR data were collected for the selected molecular join P_4Se_3-As_4Se_3 glasses using a Bruker Advance spectrometer operating at 11.7 T (Larmor frequency of 95.5 MHz and 202.4 MHz for ^{77}Se and ^{31}P, respectively). For all ^{77}Se MAS spectra, samples were crushed and packed into 4 mm ZrO_2 rotors and were spun at 12.5 kHz. A Hahn echo pulse sequence ($\pi/2-\tau-\pi-$acquisition) was employed for spectral acquisition with a $\pi/2$ pulse length of 2.75 μs and τ = 60 μs. A recycle delay of 30 s was used and approximately 500 transients were averaged and Fourier transformed to obtain each spectrum.

For all 2D ^{31}P PASS NMR experiments, crushed samples were taken either in 4 or 2.5 mm ZrO_2 rotors and were spun at 6 or 28 kHz, respectively. The PASS pulse sequence consisted of a $\pi/2$ pulse (1.95 μs) followed by a train of π pulses. The inter-pulse delays were rotor synchronized according to the solutions of the PASS equations given by Antzutkin et al. [32] All pulses were cogwheel phase cycled to eliminate the effects of pulse imperfections. The 2D acquisition consisted of 16 or 4 t_1 increments, each with 12 transients, and a recycle delay of 20 s was used.

All ^{77}Se and ^{31}P NMR spectra were externally referenced by recording the ^{17}O signal of natural abundance H_2O and using the appropriate frequency ratios as reported in the IUPAC recommendations [33].

The isotropic and anisotropic spectral line shapes, as obtained from the PASS data, were simulated using the software program DMFit to obtain the relative fractions of the various P environments and their corresponding chemical shift anisotropy (CSA) parameters [34]. The ^{31}P CSA tensors reported here follow the Haeberlen convention[35] defined as:

$$|\delta_{zz} - \delta_{iso}| \geq |\delta_{xx} - \delta_{iso}| \geq |\delta_{yy} - \delta_{iso}|,$$

$$\delta_{iso} = \frac{1}{3}(\delta_{zz} + \delta_{xx} + \delta_{yy}),$$

$$\Delta = \delta_{zz} - \delta_{iso},$$

$$\eta = \frac{\delta_{yy} - \delta_{xx}}{\Delta},$$

where δ_{xx}, δ_{yy}, and δ_{zz} are the principal components of the chemical shift tensor, the magnitude of the CSA is Δ, and its asymmetry is denoted as η, and δ_{iso} is the isotropic chemical shift.

3. RESULTS AND DISCUSSION

The ^{77}Se MAS NMR spectra of select P_4Se_3-As_4Se_3 glasses are shown in Figure 1 and are compared with the ^{77}Se MAS NMR spectrum of the P_5Se_3 glass reported by us in a recent study [13]. Two resonances centered at isotropic chemical shifts δ_{iso} ~ 800 ppm and ~ 500 ppm can be clearly identified for the As_4Se_3 glass. The resonance at ~800 ppm can be assigned on the basis of previous studies to Se atoms bonded to an apical and a basal As atom in the As_4Se_3 molecules [16,17,30]. On the other hand, the resonance at ~500 ppm was shown in these studies to be a composite peak with components at ~600 and 400 ppm, corresponding, respectively, to Se-**Se**-As

and As-**Se**-As sites in the As-Se network [16,17,30]. Progressive addition of P_4Se_3 to As_4Se_3 results in a splitting of the molecular peak at ~ 800 ppm into at least two partially resolved resonances located at δ_{iso} ~ 845 ppm and 770 ppm (Figure 1). These resonances most likely correspond to Se atoms bonded to various combinations of apical and basal P and As atoms in mixed-atom $P_xAs_{4-x}Se_3$ molecules as shown in Figure 2. Moreover, the relative intensity of the resonance at ~845 ppm increases with increasing P_4Se_3 content, which is consistent with the observation that the ^{77}Se resonance for the P(apical)-**Se**-P(basal) site in the P_4Se_3 molecules in P_5Se_3 glass is located at δ_{iso} ~ 830 ppm (Figure 1). Besides the formation of $P_xAs_{4-x}Se_3$ molecules, the addition of P_4Se_3 to As_4Se_3 results in a progressive lowering of the relative intensity of the ^{77}Se resonance at ~500 ppm corresponding to the network moieties compared to the intensity of the resonances corresponding to the molecular moieties. The results of previous ^{77}Se NMR spectroscopic studies of binary As-Se and P-Se glasses suggest that, in Se-deficient glasses such as these, both As and P atoms primarily exist in three-coordinated environments, which can form corner-shared $As(Se,As)_3$ and $P(Se,P)_3$ pyramids in the network moieties (Figure 2) and $(As/P)_4Se_3$ cage-like molecules in Se-deficient compositions [13,16]. The molecular fraction maximizes near ~ 40 atom% Se in compositions close to the $(As/P)_4Se_3$ stoichiometry. However, it is clear from the ^{77}Se NMR spectra in Figure 1 that the molecule : network fraction in glasses along the P_4Se_3 - As_4Se_3 join continuously increases on replacement of As by P.

While ^{77}Se NMR results provide information on the compositional evolution of the total molecule vs. network content in the structure of P_4Se_3 - As_4Se_3 glasses, further insight into the structure can be obtained from the ^{31}P isotropic NMR spectra (Figure 3), which provide information on the relative participation of the P atoms in the network vs. molecular moieties. The ^{31}P isotropic NMR spectrum of the P_5Se_3 glass is dominated by two relatively sharp resonances at

δ_{iso} ~ 62 ppm and – 75 ppm with relative peak-area ratio of 1:3, which correspond, respectively, to the apical and basal P sites in P_4Se_3 molecules [13,24]. The addition of 30% to 40% As_4Se_3 results in the splitting of each of these two resonances into at least three components with the apical P resonances centered at δ_{iso} ~ 66, 87 and 106 ppm and the basal P resonances centered at –73, –54 and –35 ppm (Figure 3). While the resonances at ~ 66 and –73 ppm correspond to the P_4Se_3 molecules, those at higher ppm values are clearly indicative of the formation of mixed-atom $P_xAs_{4-x}Se_3$ molecules in these glasses, where P and As randomly occupy the apical and basal sites. The chemical shift tensor parameters Δ and η at and around δ_{iso} ~ 106, 87, – 35 and – 54 ppm are obtained from simulations of the corresponding spinning sideband spikelet pattern in the anisotropic dimension (Figure 4). These simulations yield average values of Δ = – 65 ± 10 ppm and η = 0.7 ± 0.1 for peaks at δ_{iso} ~ 106 and 87 ppm and Δ = 140 ± 10 ppm and η = 0.8 ± 0.1 for peaks at δ_{iso} ~ – 35 and – 54 ppm (Figure 4), which are comparable to the literature reported CSA parameters for the apical (Δ = – 76 ± 10 ppm and η = 0.6 ± 0.1) and basal (Δ = 140 ± 10 ppm and η = 0.8 ± 0.1) P sites in P_4Se_3 molecules [13,24]. In addition to these molecular resonances, the ^{31}P isotropic NMR spectra of these glasses also display a broad resonance centered at δ_{iso} ~ 130 ppm, which can be readily assigned on the basis of previous ^{31}P NMR spectroscopic studies of P-Se glasses to three-coordinated $P(Se,P)_{3/2}$ pyramidal units, which comprise the network moieties [11–13]. The compositional evolution of the intensity of this resonance in the ^{31}P NMR spectra in Figure 3 clearly indicates that a fraction of P atoms is incorporated into the pyramidal network moieties, and the relative concentration of these moieties increases monotonically with respect to that of the molecular units in the structure of these glasses with increasing As_4Se_3 content. Such a composition dependence of the molecule : network ratio is thus consistent with the ^{77}Se MAS NMR results discussed above.

Finally, the compositional evolution of the structure of these glasses, as deduced from the ^{77}Se and ^{31}P NMR spectroscopic results, is further tested for consistency against the Raman spectroscopic data reported by us in a recent study [36]. The unpolarized Raman spectra of these P_4Se_3-As_4Se_3 glasses are shown in Figure 5 and are compared with the Raman spectrum of the P_5Se_3 glass. The main vibrational bands in the P_5Se_3 glass, which is known to consist mainly of P_4Se_3 molecules, are located at ~ 133, 213, 366, and 484 cm^{-1}. These bands belong to the various intramolecular vibrational modes of the P_4Se_3 molecule [37]. On the other hand, the Raman spectrum of the As_4Se_3 glass is dominated by relatively sharp bands at 203 and 237 cm^{-1}, which can be assigned, respectively, to As clusters which consist of randomly corrugated two-dimensional sheets of three-coordinated As atoms and to the breathing mode of the basal As_3 triangle in the As_4Se_3 molecules [16]. It may be noted that such strongly localized vibrational modes tend to have large Raman scattering cross-sections and give rise to sharp bands in the spectrum. Therefore, the strong intensity of these bands may not be necessarily indicative of a correspondingly large fraction of the associated structural moieties. In addition to these sharp bands, the Raman spectrum of the As_4Se_3 glass also consists of strong but broad bands at ~ 224 and 255 cm^{-1} that correspond to the network moieties, namely the symmetric As-Se stretching in $AsSe_{3/2}$ pyramids and to Se-Se stretches in As-**Se**-Se linkages, respectively [16,17]. The Raman spectroscopic observation of these structural moieties in the As_4Se_3 glass is fully consistent with the ^{77}Se NMR spectroscopic results discussed above. The initial substitution of P for As in P_4Se_3-As_4Se_3 glasses results in a rapid decrease in the intensity of the 203 and 237 cm^{-1} bands in the Raman spectra (Figure 5) and the eventual disappearance of the former band, implying a decrease in the relative concentration of the As clusters and As_4Se_3 molecular units. Moreover, the intensity of the broad bands at ~ 224 and 255 cm^{-1} corresponding to the As-Se network moieties also

decrease with increasing P:As ratio in these glasses, while the intramolecular vibrational bands characteristic of the P_4Se_3 molecules start to appear and get stronger with progressive replacement of As with P (Figure 5). Concomitant with these changes, the Raman spectra of the binary P_4Se_3-As_4Se_3 glasses show a slight shift of the 237 cm^{-1} band characteristic of the As_4Se_3 glass to higher wavenumbers and its splitting into a partially resolved doublet at 243 and 249 cm^{-1}. It is also noteworthy that the intramolecular vibrational band at 366 cm^{-1} in the P_5Se_3 glass displays companion peaks near ~348 and 330 cm^{-1} in all binary P_4Se_3-As_4Se_3 glasses. These characteristics of the Raman spectra are strong indicators of formation of the mixed $P_xAs_{4-x}Se_3$ molecules.

When taken together, these Raman spectroscopic results are clearly consistent with the ^{77}Se and ^{31}P NMR spectroscopic results discussed above and indicate that P and As atoms can both be incorporated into the network and molecular moieties and the overall molecule:network ratio in these glasses increases monotonically with increasing P:As ratio. As the cage-like $P_xAs_{4-x}Se_3$ molecules interact with the P-As-Se pyramidal network only through weak van der Waals type forces, this increase in the overall molecule:network ratio lowers the structural connectivity. Such a structural evolution would thus be expected to lower the T_g of these glasses monotonically with increasing P:As ratio. This expectation is indeed borne out in the compositional variation of T_g of these glasses (Figure 6), which shows a rapid drop on the initial replacement of As with P up to 20 mol% P_4Se_3, beyond which a more gradual linear decrease continues up to 70 mol% P_4Se_3.

4. CONCLUSIONS

Bulk chalcogenide glasses along the compositional join P_4Se_3-As_4Se_3 are synthesized with P_4Se_3 content ranging from 0 to 70 mol%. ^{77}Se and ^{31}P NMR and Raman spectroscopic results indicate that the structure of these glasses primarily consists of isolated molecules and pyramidal

network moieties. The cage-like $P_xAs_{4-x}Se_3$ molecules in these glasses are characterized by random mixing of P and As atoms in the apical and basal sites, similar to that reported in crystalline solid solutions of P_4Se_3 and As_4Se_3. On the other hand, the network moieties consist of three-coordinated P or As atoms forming corner-shared pyramidal units that display both P-Se and As-Se heteropolar bonds and P/As-P/As metal-metal bonds. The molecule:network ratio in the structure of these glasses monotonically increases with increasing P:As ratio. The weak van der Waals interaction between the molecular and network moieties and consequent decrease in the structural connectivity give rise to a concomitant lowering of the T_g of these glasses.

ACKNOWLEDGEMENTS

This study is supported by the National Science Foundation Grant NSF-DMR 1855176. Jason A. Brown is thanked for assistance with glass synthesis.

REFERENCES

[1] K. Tanaka, K. Shimakawa, Amorphous Chalcogenide Semiconductors and Related Materials, 2nd ed., Springer Cham, 2021.

[2] P. Ma, D.-Y. Choi, Y. Yu, X. Gai, Z. Yang, S. Debbarma, S. Madden, B. Luther-Davies, Low-loss chalcogenide waveguides for chemical sensing in the mid-infrared, Opt. Express. 21 (2013) 29927.

[3] E. Guillevic, X. Zhang, T. Pain, L. Calvez, J.L. Adam, J. Lucas, M. Guilloux-Viry, S. Ollivier, G. Gadret, Optimization of chalcogenide glass in the As-Se-S system for automotive applications, Opt. Mater. 31 (2009) 1688–1692.

[4] F. Ding, Y. Yang, S.I. Bozhevolnyi, Dynamic Metasurfaces Using Phase-Change Chalcogenides, Adv. Opt. Mater. 7 (2019) 1–15.

[5] P. Sachan, R. Singh, P.K. Dwivedi, A. Sharma, Infrared microlenses and gratings of chalcogenide: Confined self-organization in solution processed thin liquid films, RSC Adv. 8 (2018) 27946–27955.

[6] S. Clima, D. Garbin, K. Opsomer, N.S. Avasarala, W. Devulder, I. Shlyakhov, J. Keukelier, G.L. Donadio, T. Witters, S. Kundu, B. Govoreanu, L. Goux, C. Detavernier, V. Afanas'ev, G.S. Kar, G. Pourtois, Ovonic Threshold-Switching Ge_xSe_y Chalcogenide Materials: Stoichiometry, Trap Nature, and Material Relaxation from First Principles, Phys. Status Solidi - Rapid Res. Lett. 14 (2020) 1900672.

[7] B. Bureau, X.H. Zhang, F. Smektala, J.L. Adam, J. Troles, H.L. Ma, C. Boussard-Plèdel, J. Lucas, P. Lucas, D. Le Coq, M.R. Riley, J.H. Simmons, Recent advances in chalcogenide glasses, J. Non. Cryst. Solids. 345–346 (2004) 276–283.

[8] J.M. Harbold, F.Ö. Ilday, F.W. Wise, J.S. Sanghera, V.Q. Nguyen, L.B. Shaw, I.D.

Aggarwal, Highly nonlinear As–S–Se glasses for all-optical switching, Opt. Lett. 27 (2002) 119.

[9] C. Xiong, E. Magi, F. Luan, A. Tuniz, S. Dekker, J.S. Sanghera, L.B. Shaw, I.D. Aggarwal, B.J. Eggleton, Characterization of picosecond pulse nonlinear propagation in chalcogenide As_2S_3 fiber, Appl. Opt. 48 (2009) 5467–5474.

[10] S.O. Kasap, K. Koughia, M. Munzar, D. Tonchev, D. Saitou, T. Aoki, Recent photoluminescence research on chalcogenide glasses for photonics applications, J. Non. Cryst. Solids. 353 (2007) 1364–1371.

[11] D.G. Georgiev, M. Mitkova, P. Boolchand, G. Brunklaus, H. Eckert, M. Micoulaut, Molecular structure, glass transition temperature variation, agglomeration theory, and network connectivity of binary P-Se glasses, Phys. Rev. B. 64 (2001) 134204.

[12] A. Bytchkov, F. Fayon, D. Massiot, L. Hennet, D.L. Price, ^{31}P solid-state NMR studies of the short-range order in phosphorus-selenium glasses, Phys. Chem. Chem. Phys. 12 (2010) 1535–1542.

[13] B. Yuan, B. Aitken, I. Hung, Z. Gan, S. Sen, Compositional Evolution of the Structure and Connectivity in Binary P-Se Glasses: Results from 2D Multinuclear NMR and Raman Spectroscopy, J. Phys. Chem. B. 125 (2021) 13057–13067.

[14] R.T. Phillips, M.K. Ellis, Microstructure of P-Se glasses and low frequency Raman scattering, J. Non. Cryst. Solids. 164–166 (1993) 135–138.

[15] A. Bytchkov, M. Miloshova, E. Bychkov, S. Kohara, L. Hennet, D.L. Price, Intermediate- and Short-Range Order in Phosphorus-Selenium Glasses, Phys. Rev. B. 83 (2011) 144201.

[16] D.C. Kaseman, I. Hung, Z. Gan, B. Aitken, S. Currie, S. Sen, Structural and Topological Control on Physical Properties of Arsenic Selenide Glasses, J. Phys. Chem. B. 118 (2014)

2284–2293.

[17] G. Yang, B. Bureau, T. Rouxel, Y. Gueguen, O. Gulbiten, C. Roiland, E. Soignard, J.L. Yarger, J. Troles, J.C. Sangleboeuf, P. Lucas, Correlation between structure and physical properties of chalcogenide glasses in the As_xSe_{1-x} system, Phys. Rev. B. 82 (2010) 195206.

[18] B.G. Aitken, GeAs Sulfide Glasses with Unusually Low Network Connectivity, J. Non. Cryst. Solids. 345–346 (2004) 1–6.

[19] D.C. Kaseman, I. Hung, Z. Gan, S. Sen, Observation of a Continuous Random Network Structure in Ge_xSe_{100-x} Glasses: Results from High-Resolution ^{77}Se MATPASS/CPMG NMR Spectroscopy, J. Phys. Chem. B. 117 (2013) 949–954.

[20] T.G. Edwards, S. Sen, E.L. Gjersing, A combined ^{77}Se NMR and Raman spectroscopic study of the structure of Ge_xSe_{1-x} glasses: Towards a self consistent structural model, J. Non. Cryst. Solids. 358 (2012) 609–614.

[21] E.L. Gjersing, S. Sen, Structure, Connectivity, and Configurational Entropy of Ge_xSe_{100-x} Glasses: Results from ^{77}Se MAS NMR Spectroscopy, J. Phys. Chem. C. 114 (2010) 8601–8608.

[22] R. Blachnik, The compounds P_4S_3, P_4Se_3, As_4S_3 and As_4Se_3 and the quaternary system P_4S_3-P_4Se_3-As_4S_3-As_4Se_3, Thermochim. Acta. 213 (1993) 241–259.

[23] S. Soyer-Uzun, S. Sen, B.G. Aitken, Network vs Molecular Structural Characteristics of Ge-Doped Arsenic Sulfide Glasses: A Combined Neutron/X-Ray Diffraction, Extended X-Ray Absorption Fine Structure, and Raman Spectroscopic Study, J. Phys. Chem. C. 113 (2009) 6231–6242.

[24] D.C. Kaseman, O. Gulbiten, B.G. Aitken, S. Sen, Isotropic Rotation vs. Shear Rlaxation in

Supercooled Liquids with Globular Cage Molecules, J. Chem. Phys. 144 (2016) 174501.

[25] A.C. Wright, B.G. Aitken, G. Cuello, R. Haworth, R.N. Sinclair, J.R. Stewart, J.W. Taylor, Neutron Studies of an Inorganic Plastic Glass, J. Non. Cryst. Solids. 357 (2011) 2502–2510.

[26] J. Li, M. Madhavi, S. Jeppson, L. Zhong, E.M. Dufresne, B. Aitken, S. Sen, R. Kukreja, Observation of Collective Molecular Dynamics in a Chalcogenide Glass: Results from X-ray Photon Correlation Spectroscopy, J. Phys. Chem. B. 126 (2022) 5320–5325.

[27] E.L. Gjersing, S. Sen, P. Yu, B.G. Aitken, Anomalously Large Decoupling of Rotational and Shear Relaxation in a Molecular Glass, Phys. Rev. B. 76 (2007) 214202.

[28] S. Sen, W. Zhu, B. Yuan, B.G. Aitken, Rheological behavior of molecular vs network chalcogenide supercooled liquids, J. Chem. Phys. 153 (2020) 134504.

[29] B. Yuan, B.G. Aitken, S. Sen, Rheology of supercooled P-Se glass-forming liquids: From networks to molecules and the emergence of power-law relaxation behavior, J. Chem. Phys. 156 (2022) 224502.

[30] G. Yang, O. Gulbiten, Y. Gueguen, B. Bureau, J.-C. Sangleboeuf, C. Roiland, E.A. King, P. Lucas, Fragile-strong behavior in the As_xSe_{1-x} glass forming system in relation to structural dimensionality, Phys. Rev. B - Condens. Matter Mater. Phys. 85 (2012) 144107.

[31] V. Kovanda, M. Vlček, H. Jain, Structure of As-Se and As-P-Se glasses studied by Raman spectroscopy, J. Non. Cryst. Solids. 326–327 (2003) 88–92.

[32] O.N. Antzutkin, S.C. Shekar, M.H. Levitt, Two-Dimensional Sideband Separation in Magic-Angle-Spinning NMR, J. Magn. Reson. Ser. A. 115 (1995) 7–19.

[33] R.K. Harris, E.D. Becker, S.M. Cabral De Menezes, R. Goodfellow, P. Granger, NMR nomenclature: Nuclear spin properties and conventions for chemical shifts (IUPAC

recommendations 2001), Pure Appl. Chem. 73 (2001) 1795–1818.

[34] D. Massiot, F. Fayon, M. Capron, I. King, S. Le Calvé, B. Alonso, J.O. Durand, B. Bujoli, Z. Gan, G. Hoatson, Modelling one- and two-dimensional solid-state NMR spectra, Magn. Reson. Chem. 40 (2002) 70–76.

[35] U. Haeberlen, High Resolution NMR in Solids Selective Averaging: Supplement 1 Advances in Magnetic Resonance, Elsevier, 2012.

[36] B. Yuan, B.G. Aitken, S. Sen, Viscoelastic behavior and fragility of Se-deficient chalcogenide liquids in As-P-Se system, J. Non-Crystalline Solids X. 16 (2022) 100128.

[37] R.T. Phillips, D. Wolverson, M.S. Burdis, Y. Fang, Observation of discrete molecular structures in glassy P_xSe_{1-x} by Raman spectroscopy, Phys. Rev. Lett. 63 (1989) 2574–2577.

Figure Captions

Figure 1. ^{77}Se MAS NMR spectra of P_4Se_3-As_4Se_3 glasses collected at 11.7 T. Glass compositions are listed alongside the spectra. ^{77}Se MAS NMR spectrum of P_5Se_3 glass is taken from [13] and is shown here for comparison. This spectrum was collected at 19.6 T with a spinning speed of 10 KHz.

Figure 2. Cartoon showing network and molecular moieties in the structure of P_4Se_3-As_4Se_3 glasses.

Figure 3. ^{31}P isotropic NMR projections of P_4Se_3-As_4Se_3 glasses collected at 11.7 T. Glass compositions are noted alongside the spectra.

Figure 4. Experimental (empty red circles) and simulated (black traces) ^{31}P NMR spinning sideband intensity in the anisotropic dimension for (a) apical and (b) basal P sites in $P_xAs_{4-x}Se_3$ molecules in $(P_4Se_3)_{70}$ $(As_4Se_3)_{30}$ glass.

Figure 5. Unpolarized Raman spectra of P_5Se_3 and P_4Se_3-As_4Se_3 glasses. Glass compositions are listed alongside the spectra.

Figure 6. Compositional variation of glass transition temperature T_g of P_4Se_3-As_4Se_3 glasses.

Fig. 1

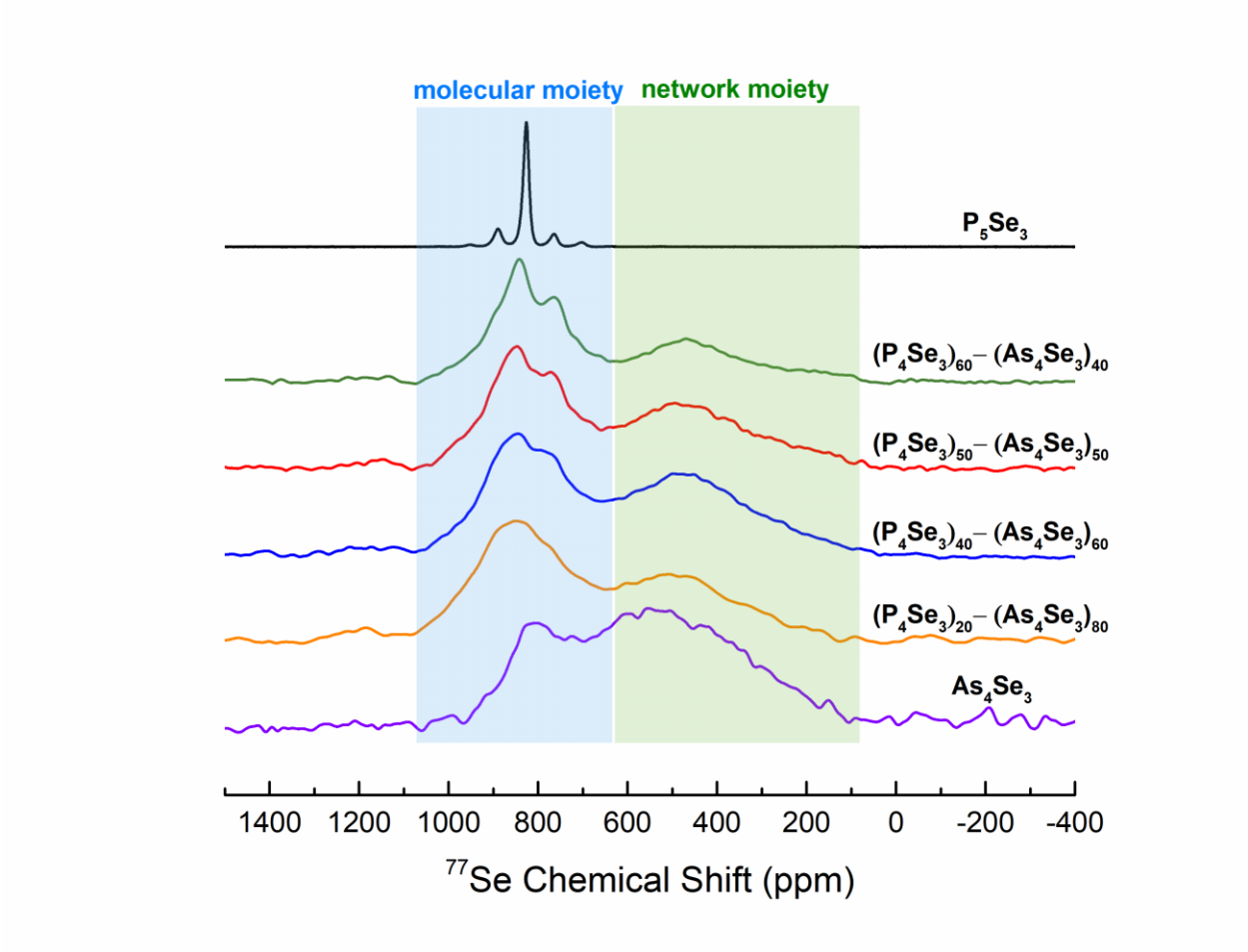
molecular moiety
network moiety
P5Se3
(P4Se3)60– (As4Se3)40
(P4Se3)50– (As4Se3)50
(P4Se3)40– (As4Se3)60
(P4Se3)20– (As4Se3)80
As4Se3
1400
1200
1000
800
600
400
200
0
-200
-400
77Se Chemical Shift (ppm)

Fig. 2

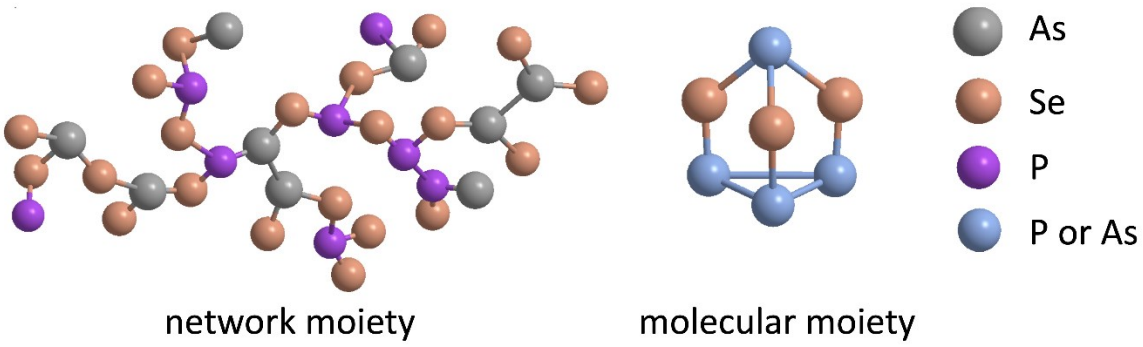

Fig. 3

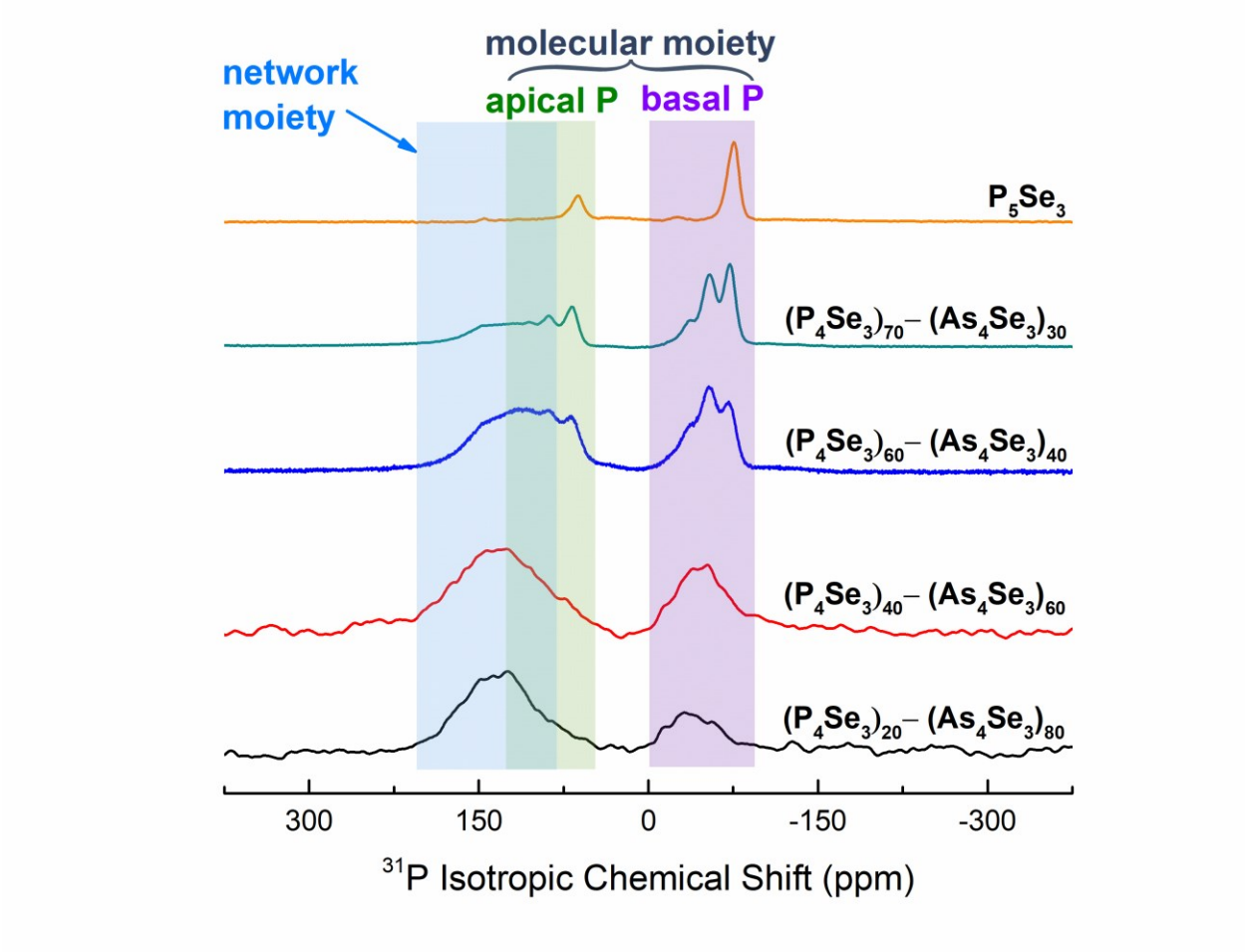
molecular moiety
network moiety
apical P
basal P
P5Se3
(P4Se3)70– (As4Se3)30
(P4Se3)60– (As4Se3)40
(P4Se3)40– (As4Se3)60
(P4Se3)20– (As4Se3)80
300
150
0
-150
-300
31P Isotropic Chemical Shift (ppm)

Fig. 4

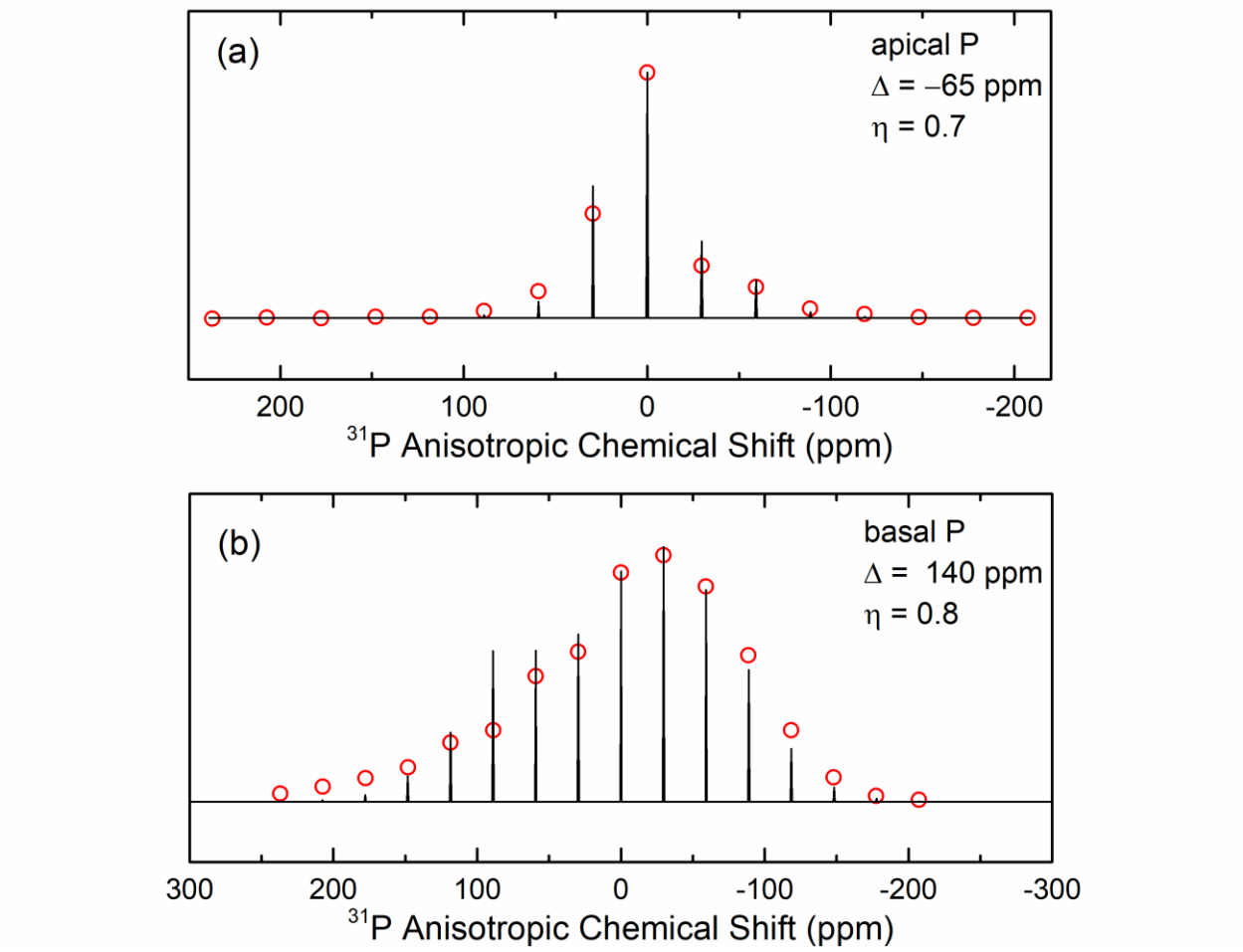
(a)
apical P
Δ = –65 ppm
η = 0.7
200
100
0
-100
-200
31P Anisotropic Chemical Shift (ppm)
(b)
basal P
Δ = 140 ppm
η = 0.8
300
200
100
0
-100
-200
-300
31P Anisotropic Chemical Shift (ppm)

Fig. 5

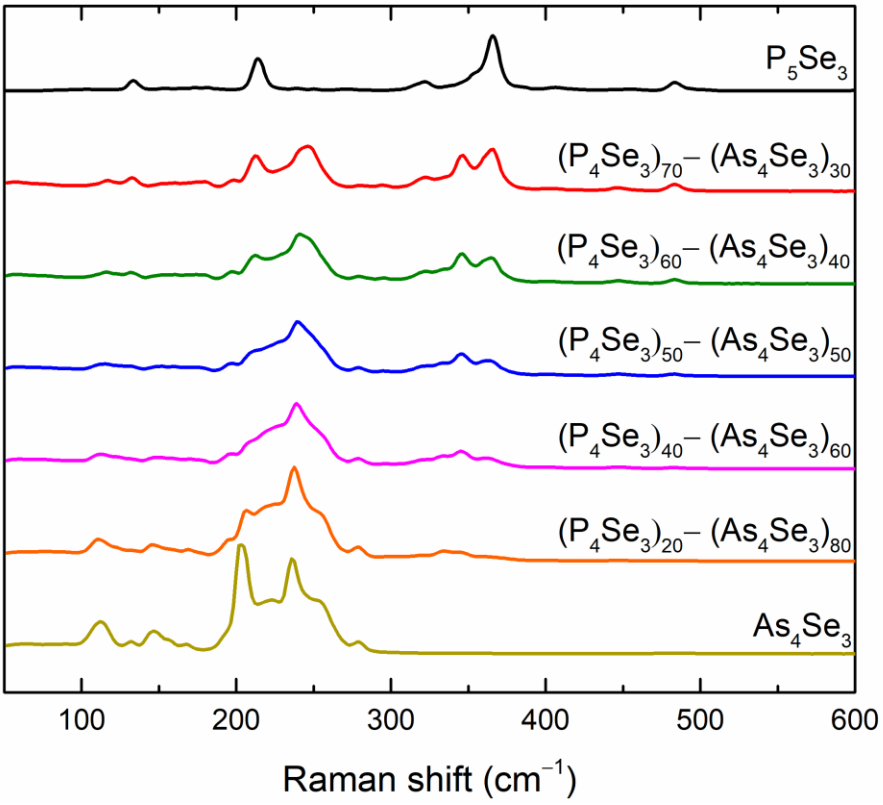
P_5Se_3
$(P_4Se_3)_{70}-(As_4Se_3)_{30}$
$(P_4Se_3)_{60}-(As_4Se_3)_{40}$
$(P_4Se_3)_{50}-(As_4Se_3)_{50}$
$(P_4Se_3)_{40}-(As_4Se_3)_{60}$
$(P_4Se_3)_{20}-(As_4Se_3)_{80}$
As_4Se_3
100
200
300
400
500
600
Raman shift (cm^{-1})

Fig. 6

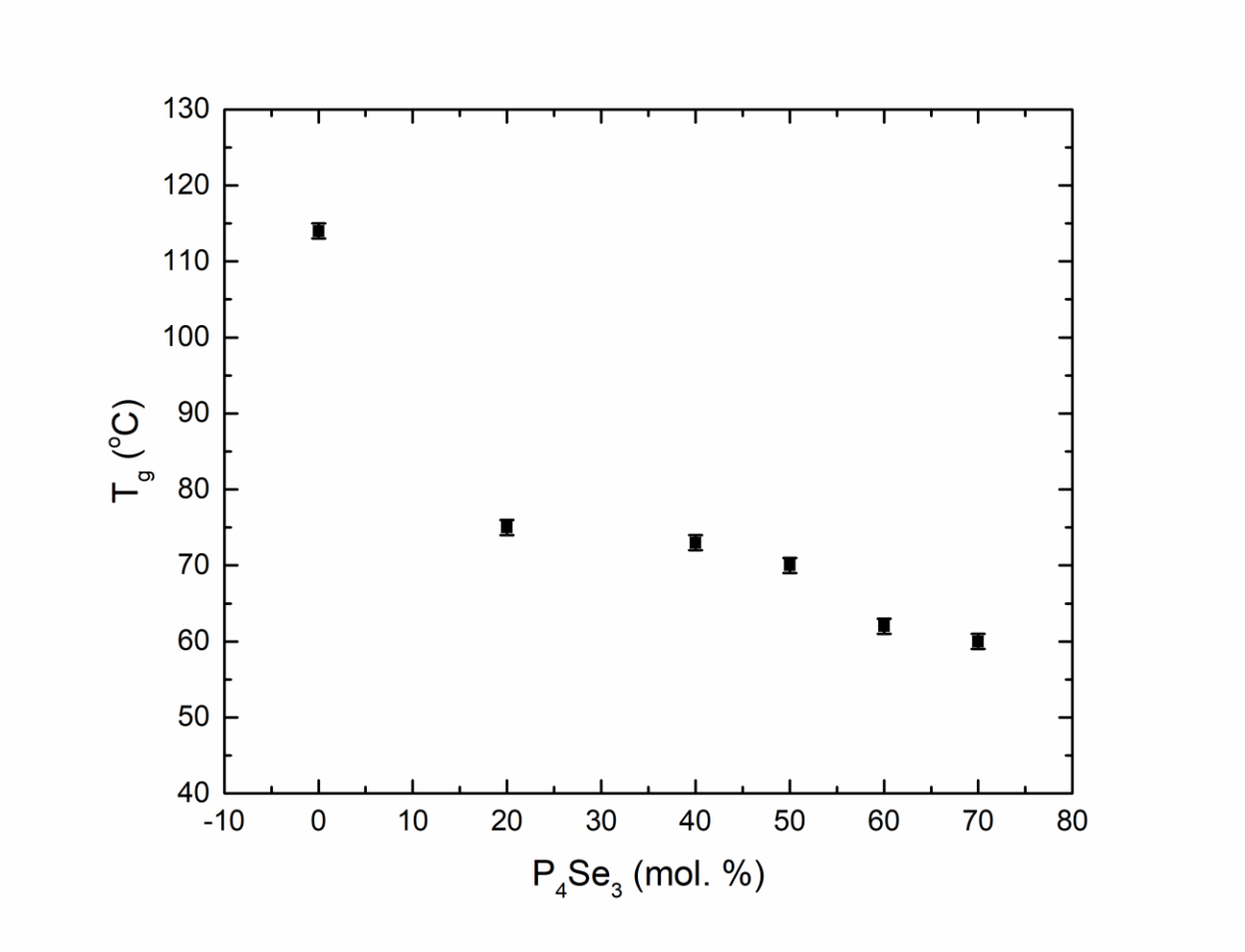
130
120
110
100
90
80
70
60
50
40
T_g (°C)
-10
0
10
20
30
40
50
60
70
80
P_4Se_3 (mol. %)